

Impact of elasticity on the piezoresponse of adjacent ferroelectric domains investigated by scanning force microscopy

Tobias Jungk,* Ákos Hoffmann, and Elisabeth Soergel
*Institute of Physics, University of Bonn,
 Wegelerstraße 8, 53115 Bonn, Germany*

(Dated: December 25, 2021)

As a consequence of elasticity, mechanical deformations of crystals occur on a length scale comparable to their thickness. This is exemplified by applying a homogeneous electric field to a multi-domain ferroelectric crystal: as one domain is expanding the adjacent ones are contracting, leading to clamping at the domain boundaries. The piezomechanically driven surface corrugation of micron-sized domain patterns in thick crystals using large-area top electrodes is thus drastically suppressed, barely accessible by means of piezoresponse force microscopy.

PACS numbers: 68.35.Ja, 68.37.Ps, 77.65.-j, 77.84.-s

I. INTRODUCTION

Ferroelectric domain patterns are intensively investigated due to their increasing practical importance, e.g. for frequency conversion [1], electrically controlled optical elements [2], photonic crystals [3] or high-density data storage [4]. For their characterization a visualization technique with high lateral resolution is required. Among a wealth of techniques [5] piezoresponse force microscopy (PFM) has become a standard tool for visualizing micron-sized domain structures. For PFM a scanning force microscope is operated in contact mode with an alternating voltage applied to the tip. In ferroelectric samples this voltage causes thickness changes via the converse piezoelectric effect [6] and therefore vibrations of the surface which lead to oscillations of the cantilever that can be read out with a lock-in amplifier [7, 8]. Quantitative analysis of PFM images is complicated by the strongly inhomogeneous electric field generated by the tip [9]. A possibility to overcome this difficulty consists in the application of large-area electrodes on the sample surfaces, thereby generating a plane plate capacitor-like electric field configuration inside the sample.

PFM with large-area top electrodes has been realized on piezoceramic thin films [10, 11, 12]. The lateral resolution was not observed to be affected by this electrode configuration. This is plausible as mechanical coupling between adjacent grains in ceramics can be assumed to be weak. Therefore they can deform independently according to their crystallographic orientation and thus their piezoelectric tensor elements. Indeed, there is no report so far on PFM measurements of differently orientated domains within a single grain covered by a metal layer. This, however, corresponds to the situation of a metalized multi-domain single crystal.

Unfortunately, there is no analytical solution to the problem of crystal deformation at a domain boundary

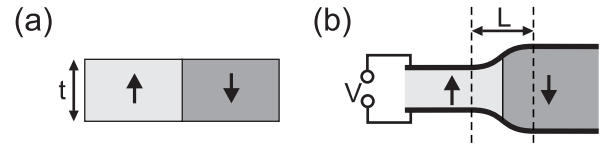


FIG. 1: (a) Bi-domain crystal of thickness t and its deformation (b) taking place on the length scale L when applying a homogeneous electric field to it. Note that the width of the domain wall itself is not affected by the deformation of the crystal.

in a homogeneous electric field taking clamping into account. However, it can be estimated from elasticity theory [13] and from finite element calculations [14] that clamping affects the surface distortion on a length scale on the same order of magnitude as the thickness of the crystal. This is exemplified in Fig. 1 where the deformation of a bi-domain crystal of thickness t in a homogeneous electric field is shown schematically.

In this contribution we investigate the impact of elasticity on the surface corrugation of multi domain samples. Due to their wide applicability we used lithium niobate (LiNbO_3) crystals exhibiting 180° domains only. The width of the domain walls is expected to be a few unit cells [15]; from high-resolution electron microscopy images they are known to be narrower than 3 nm [16]. When imaging domain walls with PFM, however, they appear to be wider due to the limited resolution of PFM, typically in the order of 50 nm [17].

II. EXPERIMENTAL PROCEDURE

For the investigations we used a commercial scanning force microscope (SMENA, NT-MDT), modified to allow the application of voltages to the tip ($10 V_{pp}$, ~ 30 kHz). All PFM images were recorded from the X -output of a dual-phase lock-in amplifier (SRS 830), thus being unaffected by the background inherent to PFM measurements [18]. The experiments were carried out with z -

*Electronic address: jungk@uni-bonn.de

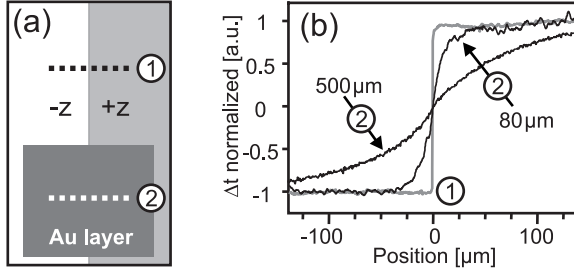


FIG. 2: (a) Diagram of the LiNbO₃ samples used to determine the surface distortion across the domain boundary with and without an additional Au-layer. (b) Line scans recorded at the positions indicated in (a) perpendicular to the domain boundary for two samples of 500 μm and 80 μm thickness. At the non-covered area the line scans ① coincide for both crystals. Δt : normalized surface deformation of the sample.

cut LiNbO₃ crystals (thicknesses: 500 μm and 80 μm). The crystals either had one domain boundary or they were periodically poled (PPLN). We partly metallized the samples with gold (Au) or copper (Cu) layers of 30 – 50 nm thickness; one sample was covered with a Cu-layer of 6 nm thickness only. Structured metal layers were fabricated using electron microscopy grids as masks for the evaporation. All samples were grounded at the back-side by a homogenous metal electrode and mounted on a piezomechanically driven translation stage with a travel range of 300 μm .

We used cantilevers from MikroMasch, some of them conductively coated with Ti-Pt. To determine the quality of the electrical connection between tip and metal layer, we applied an alternating voltage to the tip and recorded the voltage at the layer via lock-in amplification while scanning the sample. The obtained images show the connectivity between tip and metal layer. For the non-coated, highly n-doped silicon tips no electrical connection was found (most probably because of a naturally growing oxide layer of some nm thickness [19]). However, also for Ti-Pt coated tips, electrical contact for both the Au- and the Cu-layers was not reliable. This may be caused by the extremely small contact area. Hence, if the application of voltages to the metal layer was desired, we directly connected the voltage source with an extra wire.

III. EXPERIMENTAL RESULTS

A. Clamping at a single domain wall

To demonstrate the effect of clamping between adjacent 180° domains, we partly metallized two bi-domain crystals of thicknesses 500 μm and 80 μm with a 50 nm Au-layer on an area of several mm² (Fig. 2(a)). Then we measured the length of the deformation of the surface across the domain boundary with ② and without ① the Au-layer. In Fig. 2(b) line scans of 260 μm length at the

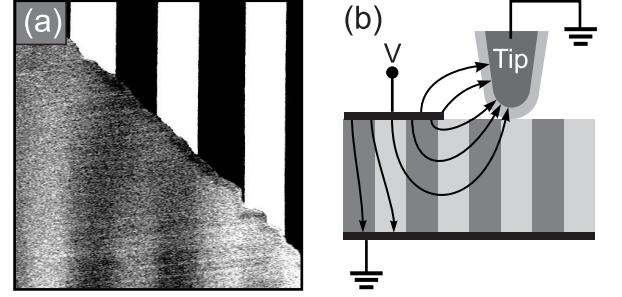


FIG. 3: (a) PFM image of PPLN partially covered with a conducting (30 nm thick) Cu-layer. The alternating voltage was applied to the Cu-layer, the tip and the back-electrode being grounded (b). The contrast in (a) is enhanced to reveal the surface corrugation under the electrode of ~ 2 pm amplitude. The image size is $25 \times 25 \mu\text{m}^2$.

positions indicated in (a) are shown. For better comparability the line scans are normalized to the same maximum crystal deformation. As the full deformation for the 500 nm thick sample was not achieved within the scan range, we measured the crystal response some mm away from the domain boundary and fitted the line scan with a modified hyperbolic tangent to estimate the width of the surface deformation [17]. Independent of the thickness of the sample, the surface distortion for both crystals using standard PFM (with the tip acting as electrode) show step-like profiles ①. On the metallized region, however, the deformation of the crystal reaches its maximum at a distance of $\sim 300 \mu\text{m}$ away from the domain boundary for the 500 μm thick crystal and at $\sim 35 \mu\text{m}$ for the 80 μm thick crystal, respectively. The surface deformation across the domain boundary is thus of the same order of magnitude as the thicknesses of the crystals. This is what can be expected from elasticity theory due to clamping between adjacent domains [13].

B. Impact of clamping on PFM imaging

To investigate the impact of clamping on the surface corrugation of multi-domain crystals, we partly metallized a 500 μm thick PPLN crystal (period $\Lambda = 8 \mu\text{m}$) with a 30 nm thick Cu-layer. Figure 3 shows a recorded PFM image with the corresponding sample configuration and electrical connection scheme. To avoid a short circuit between the grounded tip and the Cu-layer, we used a non-coated silicon tip, exhibiting a few nm-thick insulating oxide layer. The PFM measurements (Fig. 3(a)) revealed a piezomechanically driven surface deformation of 140 pm in the non-metallized part of the sample. However, underneath the Cu-layer the surface corrugation was measured to be < 2 pm. The latter result can be compared to the slope of the line scan for the 500 μm thick crystal in Fig. 2(b) which was found to be $\sim 0.4 \text{ pm}/\mu\text{m}$ at the domain boundary. The distance between neighboring domain boundaries in this PPLN crystal is 4 μm .

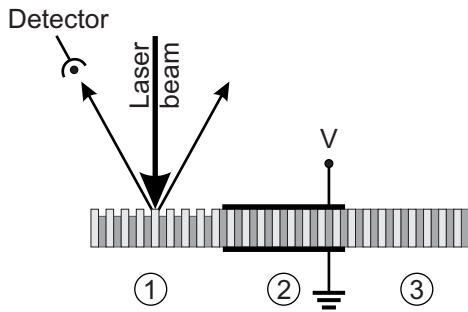


FIG. 4: Schematics of the PPLN sample used for the optical diffraction experiments. In section ① a distinct surface relief grating was obtained by etching with hydrofluoric acid, in the central section ② Au-electrodes allow the application of up to 1 kV to the sample, and section ③ remained unchanged to perform the experiments with liquid electrodes.

Therefore a surface corrugation of ~ 1.6 pm is expected which matches fairly well the measured data. This result is consistent with the assumption that the surface corrugation is reduced by a factor of $\Lambda/2t$ for periodically clamped samples, with t being the thickness of the sample [20]. The shape of the surface grating in the homogeneous electric field was found to be sinusoidal.

Furthermore, it is striking that the contrast in the two parts of the image is inverted. This becomes evident, however, when looking at the direction of the electric field inside the crystal (Fig. 3(b)). Analyzing carefully the image, it can also be observed that near the edge of the Cu-layer the contrast is reduced even more. This can be explained as follows: when the tip is at the edge of the layer, the crystal is not only clamped because of the PPLN structure underneath but in addition the non-covered part of the crystal remains undeformed because of the absence of the electrical field.

C. Optical diffraction experiments

To sustain these results and to exclude possible artifacts in the PFM measurements, we performed optical diffraction experiments [20, 21] with the surface-relief grating. Therefore an identical PPLN sample ($\Lambda = 8 \mu\text{m}$, thickness $500 \mu\text{m}$) was prepared as follows (Fig. 4): one part of the sample was etched with hydrofluoric acid to reveal the domain structure as a distinct surface-relief grating, one part of the sample was covered with a 50 nm thick Au-electrodes and the rest of the sample remained unchanged.

In a first step the exact read-out angle for the diffraction was determined with the etched part of the sample. Then the sample was moved with a translation stage in order to irradiate the part covered with the Au-electrodes. Although applying 1 kV to them, we could not observe any diffracted laser beam. We repeated the experiment with the sample mounted in a special holder with liquid electrodes [22], applying 10 kV to it. In this

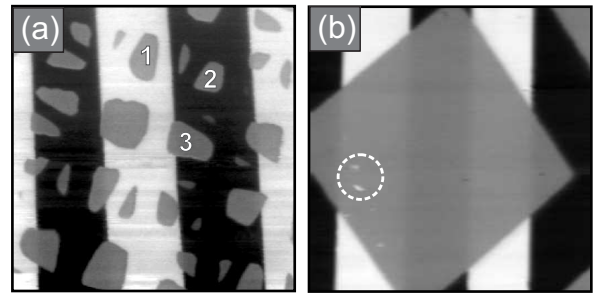


FIG. 5: Effect of isolated metal layers on PFM imaging. (a) PPLN crystal covered with Cu-islands (40 nm thickness). The size of the islands varies from $2 \mu\text{m}^2$ to $70 \mu\text{m}^2$. Some of them are located on a positive (1) or on a negative domain face only (2) and some lie across a domain boundary (3). The image size is $50 \times 50 \mu\text{m}^2$. (b) PFM image of a PPLN crystal partly covered with a 6 nm thick Cu-layer. Inside the circle the Cu-layer has defects. The image size is $60 \times 60 \mu\text{m}^2$, the full z -range of the images is 140 pm.

setup the unmodified part of the sample was investigated, thereby excluding any mechanical restriction of the Au-layer. However, also in this case no diffraction from the piezomechanically induced surface-relief grating was observed. According to the piezoelectric coefficient $d_{33} = 8.1 \text{ pm/V}$ [23] without considering clamping, a surface corrugation of ~ 80 nm should emerge when applying 10 kV to the crystal, easily detectable by optical means. We attribute the missing diffraction the extremely smoothed surface relief grating caused by clamping. This is in agreement with the results from our PFM measurements, performed with a PPLN crystal with same period Λ : Clamping reduces the piezomechanically driven surface corrugation by a factor of ~ 70 . Therefore, although applying 10 kV to the crystal, the expected surface modulation is only ~ 1 nm. The detection of such small surface corrugations, however, requires a more sophisticated setup [20] and is beyond the scope of our experimental setup.

D. Influence of metallic islands on PFM imaging

Finally, we want to underline the importance of a reliable electrical connection to the metal layer. Thus, we performed a series of experiments avoiding any connection deliberately. In this situation the metallization acts like a shield and therefore no electric field penetrates into the crystal. Consequently no PFM signal at all can be detected under the electrode. This is shown in Fig. 5(a) where 40 nm thick μm -sized Cu-islands have been deposited on top of a PPLN crystal. Some of the islands are placed at one domain face only (1 and 2), whereas others lie across a domain boundary (3). Independent on their position relative to domain boundaries no contrast can be detected under the metallic islands. The missing contrast has nothing to do with a size effect of

the electrode and therefore a changed field distribution inside the crystal [9]. Note that the PFM signal from the islands is the exact median of the two PFM signals from the $+z$ and the $-z$ domain faces. This is consistent with the system-inherent background described previously [7].

To give further evidence that the missing contrast at the Cu-islands in Fig. 5(a) is due to a shielding mechanism, we evaporated a very thin Cu-layer (6 nm) on top of a PPLN crystal. Such thin metal layers are known to be not fully conducting [24]. Thus, the shielding by the metal layer is not perfect any more, that is why we observed a faint contrast of the domain pattern underneath the Cu-layer (Fig. 5(b)). In comparison to the gratings generated in a homogeneous electric field this grating shows a pronounced step-like profile and its amplitude is roughly 7% of the amplitude measured at the non-coated area. Note that at some positions, e.g. the ones indicated with the circle in Fig. 5(b) the Cu-layer is damaged and therefore the full PFM signal can be observed.

IV. CONCLUSIONS

We have investigated the consequences of elasticity on the clamping between adjacent ferroelectric domains.

Thereby we could confirm theoretical predictions on the length scale clamping affects the surface deformation and its dependence on the thickness of the crystal. The effects being too small to be detected by optical means, we used piezoresponse force microscopy (PFM) capable of measuring deformations of only a few picometers. The obtained results have also a direct impact for the technique of PFM itself, quantifying the drawback for the resolution using a top metal layer when investigating multi-domain crystals.

Acknowledgments

We thank Michael Kösters for the optical measurements and the poling of the bi-domain samples. Many thanks also to Boris Sturman for helpful discussions. Financial support of the DFG research unit 557 and of the Deutsche Telekom AG is gratefully acknowledged.

-
- [1] M. M. Fejer, G. A. Magel, D. H. Jundt, and R. L. Byer, *IEEE J. Quantum Elect.* **28**, 2631 (1992).
 - [2] R. W. Eason, A. S. Boyland, S. Mailis, and P. G. R. Smith, *Opt. Commun.* **197**, 201 (2001).
 - [3] N. G. R. Broderick, G. W. Ross, H. L. Offerhaus, D. J. Richardson, and D. C. Hanna, *Phys. Rev. Lett.* **84**, 4345 (2000).
 - [4] Y. Cho, S. Hashimoto, N. Odagawa, K. Tanaka, and Y. Hiranaga, *Appl. Phys. Lett.* **87**, 232907 (2005).
 - [5] E. Soergel, *Appl. Phys. B* **81**, 729 (2005).
 - [6] R. E. Newnham, *Properties of Materials* (Oxford University Press, New York, 2005).
 - [7] T. Jungk, Á. Hoffmann, and E. Soergel, *Appl. Phys. Lett.* **89**, 163507 (2006).
 - [8] M. Alexe and A. Gruverman, eds., *Nanoscale Characterisation of Ferroelectric Materials* (Springer, Berlin; New York, 2004) 1st ed.
 - [9] T. Jungk, Á. Hoffmann, and E. Soergel, *Appl. Phys. A* **86**, 353 (2007).
 - [10] O. Auciello, A. Gruverman, and H. Tokumoto, *Integr. Ferroelectr.* **15**, 107 (1997).
 - [11] A. Gruverman, O. Auciello, and H. Tokumoto, *Ann. Rev. Mat. Sci.* **28**, 101 (1998).
 - [12] A. Gruverman, B. J. Rodriguez, A. I. Kingon, R. J. Nemanich, J. S. Cross, and M. Tsukada, *Appl. Phys. Lett.* **82**, 3071 (2003).
 - [13] S. P. Timoshenko and J. M. Goodier, *Theory of elasticity* McGraw-Hill international editions (1970) 3rd ed.
 - [14] T. Jach, S. Kim, V. Gopalan, S. Durbin, and D. Bright, *Phys. Rev. B* **69**, 064113 (2004).
 - [15] B. Meyer and D. Vanderbilt, *Phys. Rev. B* **65**, 104111 (2002).
 - [16] M. Foeth, A. Sfera, P. Stadelmann, and P.-A. Buffat, *J. Electron. Microsc.* **48**, 717 (1999).
 - [17] T. Jungk, Á. Hoffmann, and E. Soergel, *arXiv.org: cond-mat/0703793* (2007).
 - [18] T. Jungk, Á. Hoffmann, and E. Soergel, *J. Microsc.-Oxford* **227**, 76 (2007).
 - [19] S. M. Sze, *Semiconductor devices* (J. Wiley and Sons, 2002) 2nd ed.
 - [20] S. Stepanov, N. Korneev, A. Gerwens, and K. Buse, *Appl. Phys. Lett.* **72**, 879 (1998).
 - [21] J. Capmany, C. R. Fernández-Pousa, E. Diéguez, and V. Bermúdez, *Appl. Phys. Lett.* **83**, 5145 (1998).
 - [22] M. Müller, E. Soergel, and K. Buse, *Appl. Phys. Lett.* **83**, 1824 (2003).
 - [23] M. Jazbinšek and M. Zgonic, *Appl. Phys. B* **74**, 407 (2002).
 - [24] U. Jacob, J. Vancea, and H. Hoffmann, *Phys. Rev. B* **41**, 11852 (1990).